Communications on Applied Nonlinear Analysis
ISSN: 1074-133X
Vol 32 No. 1 (2025)

Mathematical Framework and Computational Analysis of RNA-Level Interactions Between M. tuberculosis and BCG Glaxo

Gunasekaran.M[1] , Alamelu.K[2]*

[1]PG Department of Mathematics, Sri Subramaniya Swamy Government Arts College, Tiruttani- 631 209, India.
[2]Department of Mathematics, Nazareth College of Arts and Science, Avadi, Chennai–600062, India.
[2]PG Department of Mathematics, Sri Subramaniya Swamy Government Arts College, Tiruttani- 631209, India., alameluiyappan@gmail.com

Article History:
Received: *20-11-2024*
Revised: *17-12-2024*
Accepted: *12-01-2025*

Abstract:

A well-constructed ordinary differential equation (ODE) model is an essential tool for simulating the interactions between Mycobacterium tuberculosis and Mycobacterium bovis BCG Glaxo both quantified in RNA/fg/cell. The model can be numerically solved using techniques such as the fourth-order Runge-Kutta method (RK4) or Euler's method with Python serving as an effective platform for implementation. This model enables researchers to explore the dynamics between M. tuberculosis and M. bovis BCG Glaxo across different scenarios. It allows for the assessment of how variations in parameters, initial conditions and boundary conditions impact the interaction between these microorganisms. Additionally, the model facilitates the examination of time-dependent changes in these interactions, offering valuable insights into their long-term behaviours. Furthermore, the model provides a means to compare the outcomes produced by different numerical techniques contributing to a deeper understanding of the interactions between M. tuberculosis (rna/FG/CELL) and M. bovis BCG Glaxo (RNA/fg/cell). This ODE model is a critical asset in advancing our understanding of these important bacterial interactions.

Keywords: M. tuberculosis (RNA/fg/cell), M. bovis BCG Glaxo (RNA/fg/cell), ODE model, Eulers model, RK4 method.

1. Introduction

A mathematical model is used to examine M. tuberculosis (TB) dynamics while incorporating different vaccination strategies. By utilizing differential equations, the model simulates the transmission of TB and evaluates how various vaccination control measures influence disease progression. The research offers valuable insights into the most effective vaccination strategies and their role in managing TB outbreaks [8, 22]. An advanced mathematical model is designed to analyze M. tuberculosis (TB) dynamics by integrating various intervention strategies including treatment and vaccination. Utilizing differential equations, the model effectively tracks the spread and development of TB and assesses the influence of different control measures. The results underscore the most effective strategies for decreasing TB incidence and enhancing public health [5,9]. Mycobacterium tuberculosis, the bacterium responsible for M. tuberculosis (TB) remains a leading cause of mortality worldwide with 10 million new cases and 1.2 million deaths reported in 2019 alone. Approximately 25% of the global population is estimated to carry a latent TB infection, posing a risk of developing active disease later on (WHO, 2020).

The research investigates mathematical models for the dynamics of infectious diseases, with a particular emphasis on vaccination strategies [2]. By using differential equations, the study simulates disease transmission and assesses the effects of vaccination on disease spread [6]. It offers an in-depth examination of how various vaccination approaches influence disease rates and control measures. The results underscore the essential role of vaccination in managing and reducing the impact of infectious diseases, providing crucial insights for public health strategies [4, 19]. Phylogenetic analyses have extensively explored the genomic differences between virulent strains of M. bovis and M. tuberculosis as well as the BCG vaccine strains, focusing on the remodeling of protein complexes [1, 3, 21]. However, there has been less emphasis on how genetic variability influences virulence factors related to the lipid content and metabolism of mycobacterial cell walls [1].

The metabolic processes of mycobacteria have been thoroughly studied in various academic publications [7, 15, 16, 17, 18]. During the in vitro growth of M. tuberculosis, different energy and carbon sources are channelled into major metabolic pathways where they are oxidized to produce pyruvate and eventually carbon dioxide. The Embden-Meyerhof-Parnas (EMP) pathway is the primary route for glucose catabolism in mycobacteria, with 70% of glucose entering this pathway and the remaining 30% being processed through the pentose phosphate pathway producing C5 and C4 sugars and reducing equivalents like NADPH [17]. Pathogenic mycobacteria lack alternative sugar catabolic pathways with glycerol being the preferred carbon source. The metabolic breakdown of glycerol is well-documented involving glycerol kinase and glycerol-3-phosphate dehydrogenase to eventually produce dihydroxyacetone phosphate, which is further metabolized via the EMP pathway and the Krebs cycle. Notably, a single nucleotide mutation in the pykA gene encoding pyruvate kinase, has been identified as the cause of Mycobacterium bovis's inability to utilize glycerol in the absence of pyruvate [20]. In a related context of complex biological systems, research has also focused on multispecies ecological models, examining optimal harvesting, stability dynamics and the roles of functional response, refuge, migration and immigration [10, 11, 12, 13].

2. Mathematical Model for M. tuberculosis (RNA/fg/cell) and M. bovis BCG Glaxo (RNA/fg/cell)

The density of the prey population is the variable M.T.(RNA). The predator population density and instantaneous growth rates of the two populations are represented by the variable M.BCG (RNA), where t is a time variable. The parameters of the prey α_1 and β_1 represent the maximum growth rate of the prey per capita and the impact of predators on the prey growth rate respectively. The characteristics of the predator, denoted as γ_1, δ_1 respectively, depict the rate of mortality per unit of the predator and the impact of prey on the predator's growth rate. Every parameter is actual and positive [14].

The initial conditions are α_1 = 1.

Mortality rate due to predators, β_1 = 1, δ_1 = 1, γ_1 = 2, x_0 = 232, y_0 =13.3, t=30 days, t_{max} = 2.40

$$\frac{d(M.T.(RNA))}{dt} = \alpha_1(M.T.(RNA)) - \beta_1(M.T.(RNA))(M.BCG(RNA)) \quad ...(1)$$

$$\frac{d(M.BG(RNA))}{dt} = \delta_1(M.T.(RNA)(M.BCG(RNA)) - \gamma_1(M.BCG(RNA))) \quad ...(2)$$

We obtain equation (1) and (2) two equilibrium points (0,0) and $\left(\frac{\delta_1}{\gamma_1}, \frac{\alpha_1}{\beta_1}\right)$ from equations (1) and (2). The Jacobian matrix can be used to ascertain whether these equilibrium points are stable. Each time the Jacobian is evaluated at an equilibrium point, we obtain

$$J(M.T(RNA), M.BCG(RNA) = \left(\alpha_1 + \beta_1(M.BCG(RNA)\,\beta_1(M.T(RNA)\ - \gamma_1(M.BCG(RNA)\,\delta_1 - \gamma_1(M.T(RNA)\right)$$

Every equilibrium point's Jacobian is evaluated, and the result is

$$(\alpha_1\ 0\ 0\ \delta_1\ )J\left(\frac{\delta_1}{\gamma_1}, \frac{\alpha_1}{\beta_1}\right) = \left(\alpha_1\ \beta_1\left(\frac{\alpha_1}{\beta_1}\right) - \gamma_1\left(\frac{\delta_1}{\gamma_1}\right)\ \delta_1\ \right)$$

The stability [18] of (0,0) is dependent on the signs of a and d since the eigen values of J (0,0) are $\lambda_1 = \alpha_1$and $\lambda_2 = \alpha_2$. (0,0) is a stable node if both $\alpha_1 < 0$ and $\delta_1 < 0$. If $\alpha_1 < 0$ and $\delta_1 < 0$, then the node (0,0) is unstable. A saddle point is (0,0) if $\alpha_1 < 0$ and $\delta_1 < 0$. If (0,0) is an unstable node, then δ_1>0. (0,0) is a saddle point if $\alpha_1\delta_1 < 0$. The eigenvalues of of $J\left(\frac{\delta_1}{\gamma_1}, \frac{\alpha_1}{\beta_1}\right)$ are $\lambda_1 = \alpha_1 + \frac{\beta_1}{\gamma_1}\delta_1$ and $\lambda_2 = \delta_1 - \frac{\gamma_1}{\beta_1}\alpha_1$, therefore the signs of $\alpha_1 + \frac{\beta_1}{\gamma_1}\delta_1$ and $\delta_1 - \frac{\gamma_1}{\beta_1}\alpha_1$ determine the stability of $\left(\frac{\delta_1}{\gamma_1}, \frac{\alpha_1}{\beta_1}\right)$ Since the sign of both eigenvalues is the same, $\left(\frac{\delta_1}{\gamma_1}, \frac{\alpha_1}{\beta_1}\right)$ Depending on whether the eigen values are positive or negative, it can be either a staple spiral or a tip of saddle. In the event that one eigenvalue is zero, the stability must be ascertained using higher-order terms.

3. ODE Model for M. tuberculosis (RNA/fg/cell) and M. bovis BCG Glaxo (RNA/fg/cell)

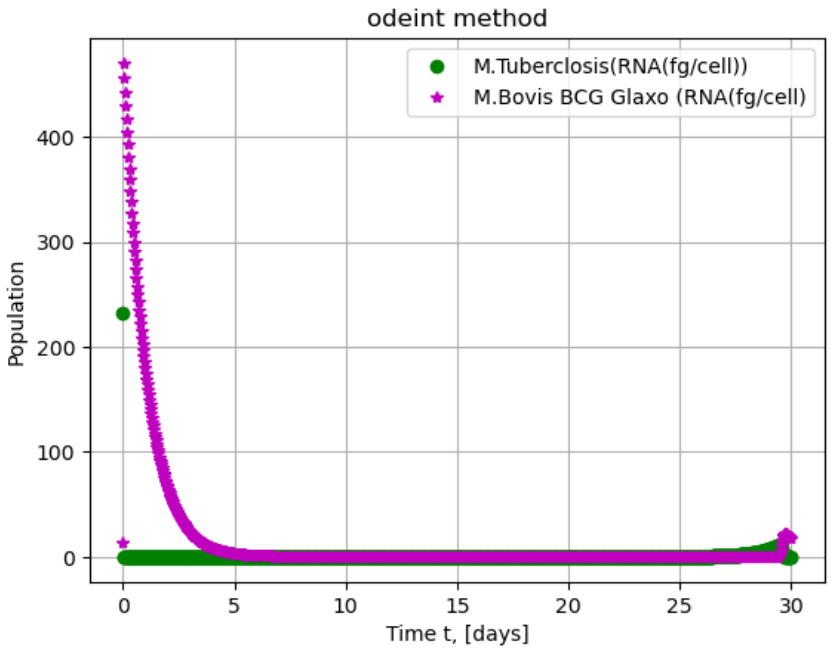

Figure 1: Interaction of ODE Model M. tuberculosis (RNA/fg/cell) and M. bovis BCG Glaxo (RNA/fg/cell)

Time t,days	M. tuberculosis (RNA/fg/cell)	M. bovis BCG Glaxo (RNA/fg/cell)
30	2.32000000e+02	1.33000000e+01
30	5.36260537e-03	4.70179582e+02
30	5.10665353e-09	4.56280426e+02
30	7.41917016e-03	1.88274550e+01
30	4.37982633e-03	1.82767912e+01
30	2.62816462e-03	1.77397467e+01

Table 1: Interaction of ODE Model M. tuberculosis (RNA/fg/cell) and M. bovis BCG Glaxo (RNA/fg/cell)

In **figure 1**, using equation (1) and (2), the population dynamics of two cell types, "M. tuberculosis (RNA/fg/cell)" and "M. bovis BCG Glaxo (RNA/fg/cell)," are plotted over a 30-day period using the Odeint method. The key observations from the plot are as follows: M. tuberculosis Population: Represented by green circles, the population of M. tuberculosis starts at around 400 and rapidly declines to nearly zero within the first five days, remaining at this low level for the rest of the period. M. bovis BCG Glaxo Population: Depicted by purple stars, the M. bovis BCG Glaxo population remains at zero throughout the entire 30-day study period. Duration: The x-axis displays the time span ranging from 0 to 30 days. Population: The y-axis represents the cell population ranging from 0 to 400. This plot can be used to study the behavior of these two cell populations over time offering insights into the dynamic interaction between these species.

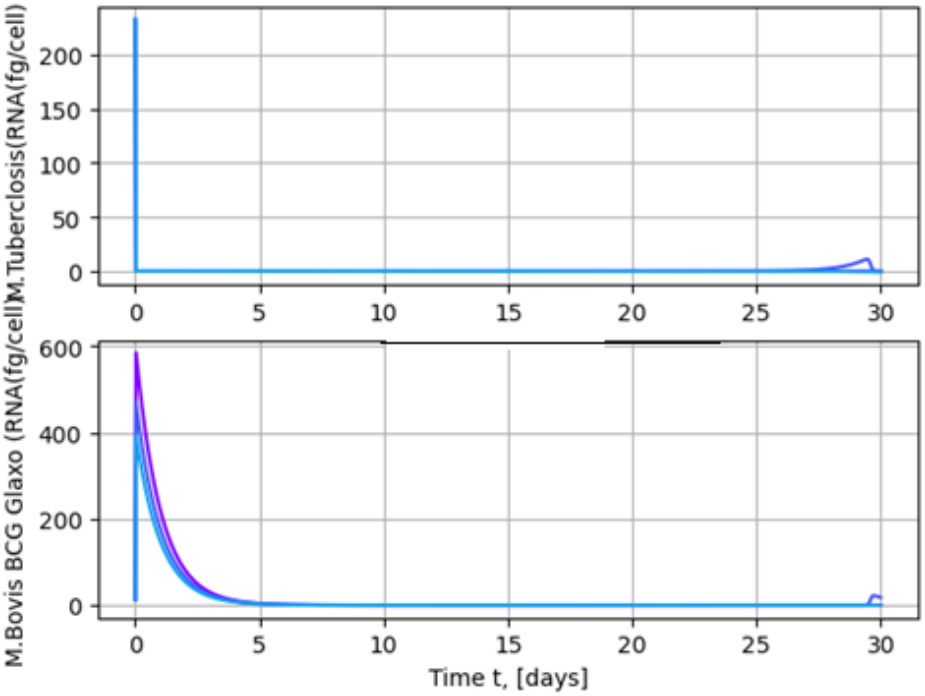

Figure 2: Interaction of Random Model M. tuberculosis (RNA/fg/cell) and M. bovis BCG Glaxo (RNA/fg/cell)

The graph illustrates the temporal variation in RNA content (fg/cell) of M. tuberculosis and M. bovis BCG Glaxo over a 30-day period. In the case of M. tuberculosis (top panel), a sharp peak in RNA levels is observed at the initial time point followed by a rapid decline to nearly negligible levels within the first day. This low level is maintained consistently throughout the observation period with a slight increase near the 30th day possibly indicating late-stage metabolic reactivation or model fluctuation. Similarly, M. bovis BCG Glaxo (bottom panel) exhibits a high initial RNA concentration that quickly diminishes within the first few days stabilizing at minimal levels thereafter. A modest rise in RNA content is also noticeable toward the end of the time frame. Overall, both strains demonstrate an early and significant reduction in RNA levels suggesting a swift transition into a low metabolic or dormant state with potential signs of late reactivation.

M. tuberculosis (RNA/fg/cell)	**M. bovis BCG Glaxo (RNA/fg/cell)**	**M. tuberculosis (RNA/fg/cell)**	**M. bovis BCG Glaxo (RNA/fg/cell)**	**M. tuberculosis (RNA/fg/cell)**	**M. bovis BCG Glaxo (RNA/fg/cell)**
2.32000000e+02	1.33000000e+01	2.32000000e+02	1.33000000e+01	2.32000000e+02	1.33000000e+01
7.15159481e-03	5.85028044e+02	5.36260537e-03	4.70179582e+02	4.18250166e-03	3.93679854e+02
7.13810820e-09	5.67738228e+02	5.10665353e-09	4.56280426e+02	3.79076358e-09	3.82040177e+02
1.44562529e-01	8.03079154e-11	7.41917016e-03	1.88274550e+01	-7.60460782e-01	8.81859962e-12
1.48969587e-01	7.86220565e-11	4.37982633e-03	1.82767912e+01	-7.83643794e-01	8.16998368e-12
1.53510998e-01	7.69922730e-11	2.62816462e-03	1.77397467e+01	-8.07533554e-01	7.55838277e-12

Table 2: Interaction of Random Model M. tuberculosis (RNA/fg/cell) and M. bovis BCG Glaxo (RNA/fg/cell)

3.1. Euler's Model for M. tuberculosis (RNA/fg/cell) and M. bovis BCG Glaxo (RNA/fg/cell)

A first-order numerical method called Euler's method can be used to solve ordinary differential equations (ODEs) starting with a given initial value. It builds the tangent at point x using the straightforward method to get the value of y(x+h), whose slope is $y'(x)$. By using the tangent at each interval that is, a series of brief line segments we can use Euler's method to approximate the solution's curve at steps of h. An increase in approximation accuracy can be achieved by using small step sizes. Given a position b and an interval width (size of each step) of h, the general formula for the functional value at any given location b is y(b).

Assuming h to be the time step, we can write:

$$y(b) = y(a) + h * \sum_{i=1}^{n} f(x_{i-1}, y_{i-1})$$

Where $x_i = x_{i-1} + h$

$$y_i = y_{i-1} + h * f(x_{i-1}, y_{i-1})$$

Here, f (x, y) is the derivative of y with respect to x.

Using equations (1) and (2), we have

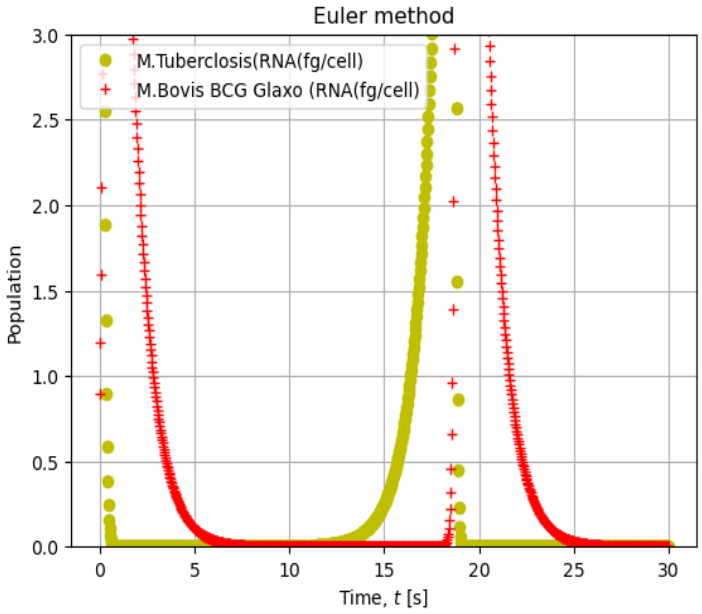

Figure 3: Interaction of Euler Model M. tuberculosis (RNA/fg/cell) and M. bovis BCG Glaxo (RNA/fg/cell)

Time t, days	M. tuberculosis (RNA/fg/cell)	M. bovis BCG Glaxo (RNA/fg/cell)
30	5.98558559e+00	1.19729730e+00
30	5.98558559e+00	1.19729730e+00
30	5.90707973e+00	1.59176437e+00
30	2.10905127e-05	2.10073104e-04
30	2.17237017e-05	2.03764869e-04
30	2.23759056e-05	1.97646069e-04

Table 3: Interaction of Euler Model M. tuberculosis (RNA/fg/cell) and M. bovis BCG Glaxo (RNA/fg/cell)

In **figure 3**, the population dynamics of two cell types, M. tuberculosis (RNA/fg/cell) and M. bovis BCG Glaxo (RNA/fg/cell), are plotted over a 30-second interval using the Euler method. M. tuberculosis (green circles): The population starts at a relatively high level and rapidly declines within the first few seconds reaching near zero around the 10-second mark. The population remains at zero until around 18 seconds, where it rapidly increases again towards the end of the period. M. bovis BCG Glaxo (red crosses): This population initially grows peaking shortly before the 5-second mark and then decreases sharply stabilizing near zero between 10 and 15 seconds. Following this period, the population begins to increase again after 18 seconds, mirroring the behavior of M. tuberculosis. Time Axis (x-axis): The time is represented from 0 to 30 seconds. Population Axis (y-axis): The population is measured ranging from 0 to 3.0 RNA/fg/cell.

Therefore, the figure suggests that both M. tuberculosis and M. bovis BCG Glaxo populations exhibit cyclical behavior with distinct phases of growth and decline. Initially, M. tuberculosis declines rapidly while M. bovis increases followed by a period where both populations stabilize near zero. After 18 seconds, both populations experience rapid growth indicating a possible interaction or competition between the two species that affects their population dynamics over time.

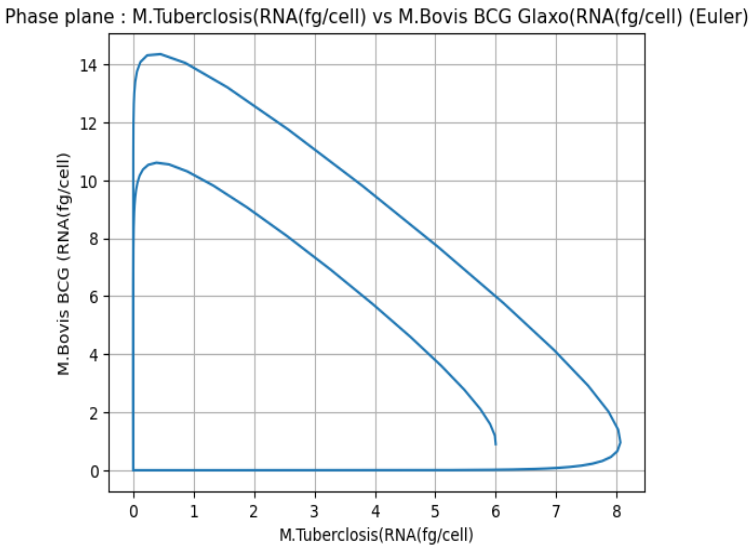

Figure 4: Phase graph of Euler Model M. tuberculosis (RNA/fg/cell) and M. bovis BCG Glaxo (RNA/fg/cell)

The **figure 4** presents a phase plane analysis of M. tuberculosis (RNA/fg/cell) against M. bovis BCG Glaxo (RNA/fg/cell) using the Euler method. The trajectories depicted in the graph suggest a non-linear relationship between the two populations over time. Cyclical Dynamics: The phase plane shows a clear cyclic pattern, indicating that the populations of M. tuberculosis and M. bovis BCG Glaxo undergo oscillations. This suggests that the interaction between these two cell types is dynamic with each population affecting the growth and decline of the other. Population Interactions: At the beginning of the cycle, when M. tuberculosis population is low, M. bovis BCG Glaxo population increases sharply. As the M. tuberculosis population starts to grow, the M. bovis population begins to decline, suggesting a competitive or inhibitory interaction. Multiple Cycles: The presence of multiple loops in the graph indicates that the system might experience repeated cycles of population growth and decline, potentially reflecting periods of dominance by one species followed by the other.

This phase plane analysis highlights the complex interplay between the two bacterial populations and provides insights into their competitive dynamics under the modelled conditions.

3.2. Runge-kutta Model for M. tuberculosis (RNA/fg/cell) and M. bovis BCG Glaxo (RNA/fg/cell)

A numerical approach for solving ordinary differential equations (ODEs) of the form dy/dx = f(x, y), y (x (0)) = y (0) is the fourth-order Runge-Kutta method. It is an improvement on the first-order Euler's approach that yields greater accuracy with fewer computations. 1. One of the most popular Runge-Kutta techniques for determining the solution to differential equation 2 is the fourth-order method. Although the RK4 approach requires more computing power, it is also more accurate than the Euler's method. Because of the method's precision and adaptability, scientific computing uses it extensively 12.

Let h be the time step, then

$$y_{i+1} = y_i + \frac{1}{6}(k_1 + 2k_2 + 2k_3 + k_4)$$

Where

$$k_1 = hf(x_i, y_i)$$

$$k_2 = hf(x_i + \frac{h}{2}, y_i + \frac{k_1}{2})$$

$$K_3 = hf(x_i + \frac{h}{2}, y_i + \frac{k_2}{2})$$

$$k_4 = hf(x_i + h, y_i + k_3)$$

Using equations (1) and (2), we have

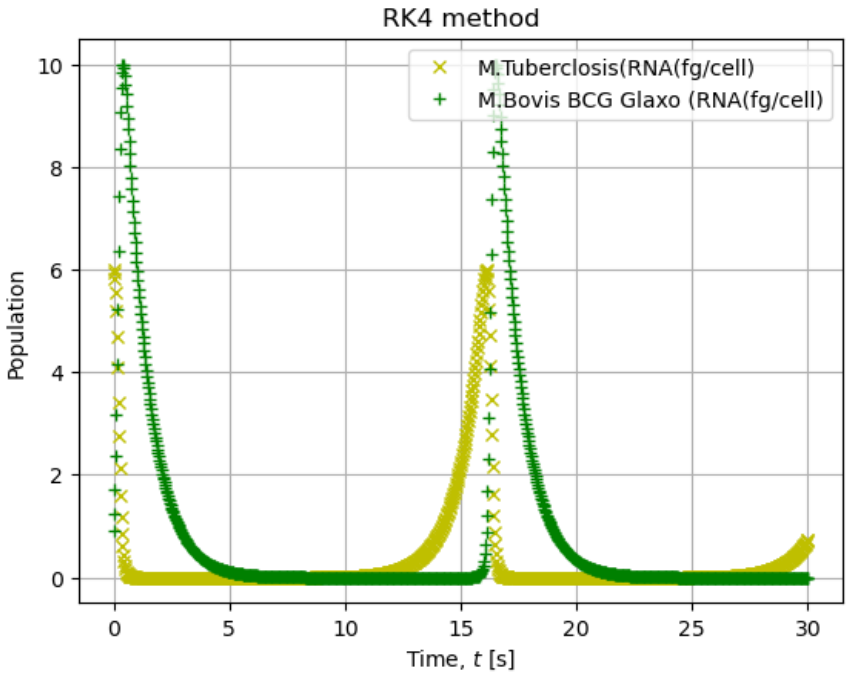

Figure 5: Interaction of RK-Method Model M. tuberculosis (RNA/fg/cell) and M. bovis BCG Glaxo (RNA/fg/cell)

Time t, days	M. tuberculosis (RNA/fg/cell)	M. bovis BCG Glaxo (RNA/fg/cell)
30	6.00000000e+00	9.00000000e-01
30	5.94990280e+00	1.25084405e+00
30	5.81328647e+00	1.72893963e+00
30	6.97317631e-01	6.52172901e-05
30	7.18573994e-01	6.60367011e-05
30	7.40478292e-01	6.69531236e-05

Table 4: Interaction of RK-method model M. tuberculosis (RNA/fg/cell) and M. bovis BCG Glaxo (RNA/fg/cell)

The **figure 5** illustrates the dynamics of two cell types: M. tuberculosis (RNA/fg/cell) and M. bovis BCG Glaxo (RNA/fg/cell) over a 30-second period analysed using the RK4 method. Key observations are as follows: M. tuberculosis Population: Represented by "x" markers, the population of M. tuberculosis increases rapidly reaches a peak and then declines sharply. M. bovis BCG Glaxo Population: Indicated by "+" markers, this population also rises quickly but peaks slightly later than M. tuberculosis before starting to decrease. Time Frame: The x-axis represents time from 0 to 30 seconds. Population Levels: The y-axis displays cell populations ranging from 0 to 10.

This figure reveals that both cell types exhibit a growth pattern followed by a decline with M. bovis BCG Glaxo peaking after M. tuberculosis. The observed patterns suggest a dynamic interplay between these populations where the growth of one influence the decline of the other.

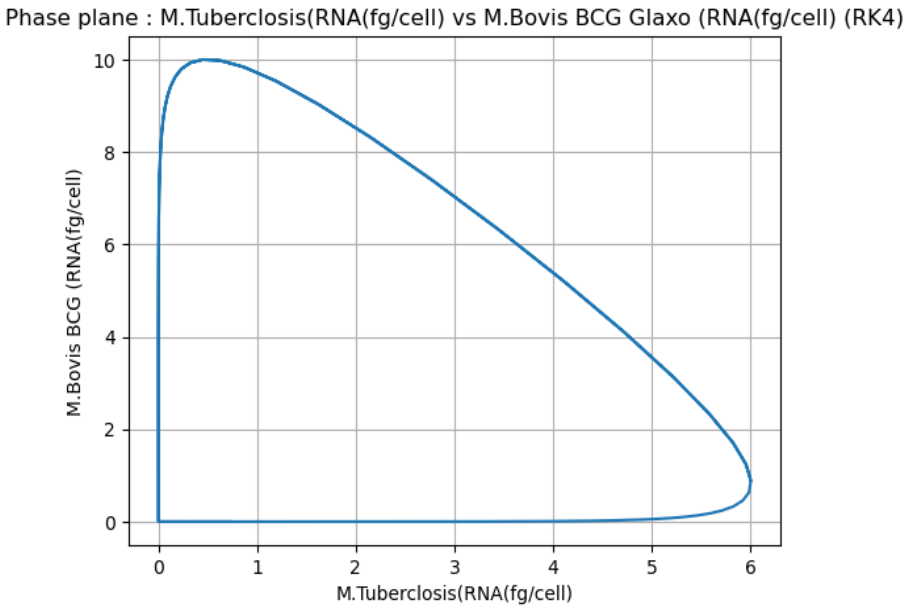

Figure 6: Interaction of RK-method model M. tuberculosis (RNA/fg/cell) and M. bovis BCG Glaxo (RNA/fg/cell)

Phase Plane Analysis: The figure 6 presents a phase plane comparison of M. tuberculosis (RNA/fg/cell) and M. bovis BCG Glaxo (RNA/fg/cell) using the RK4 method, examining their respective phases over time. Key features include: M. tuberculosis Population: Shown on the x-axis ranging from 0 to 6 reflecting the RNA per cell for M. tuberculosis. M. bovis BCG Glaxo Population: Depicted on the y-axis, ranging from 0 to 10 representing the RNA per cell for M. bovis BCG Glaxo. Phase Plane Dynamics: Starting from the origin, the blue curve rises sharply, reaches a peak around 2 on the x-axis and then gradually declines. This analysis illustrates the phase relationship between the two cell types highlighting how their populations change relative to one another over the observed period.

4. Generation Time

The tubercle bacillus known for its complex cell envelope, slow growth rate, intracellular pathogenicity, dormancy and genetic uniformity exhibits a generation time of approximately 24 hours in both infected hosts and synthetic media.

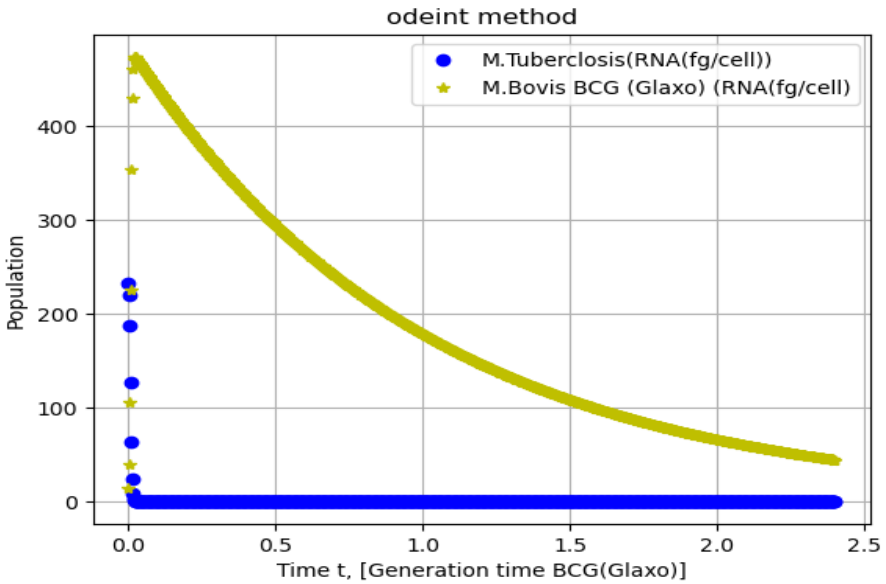

Figure 7: Interaction of ODE model M. tuberculosis (RNA/fg/cell) and M. bovis BCG Glaxo (RNA/fg/cell)

Generation Time t,days	M. tuberculosis (RNA/fg/cell)	M. bovis BCG Glaxo (RNA/fg/cell)
240	2.32000000e+02	1.33000000e+01
240	2.19437254e+02	3.94572760e+01
240	1.86785548e+02	1.05583869e+02
240	-8.10538564e-10	4.41667655e+01
240	-7.65049933e-10	4.40607865e+01
240	-7.16852963e-10	4.39550618e+01

Table 5: Interaction of ode model M. tuberculosis (RNA/fg/cell) and M. bovis BCG Glaxo (RNA/fg/cell)

The figure 7 depicting Generation Time BCG (Glaxo) illustrates the population dynamics of M. tuberculosis and M. bovis over time. The x-axis represents time spanning from 0 to 2.5, measured in Generation Time BCG (Glaxo). The y-axis displays the population of the bacteria ranging from 0 to 10. M. tuberculosis is indicated by blue circles which show a rapid increase in population followed by a decline suggesting that this bacterium eventually reaches a peak. In contrast, M. bovis BCG (Glaxo), represented by green plus markers also shows population growth but peaks later and at a lower level before beginning to decrease.

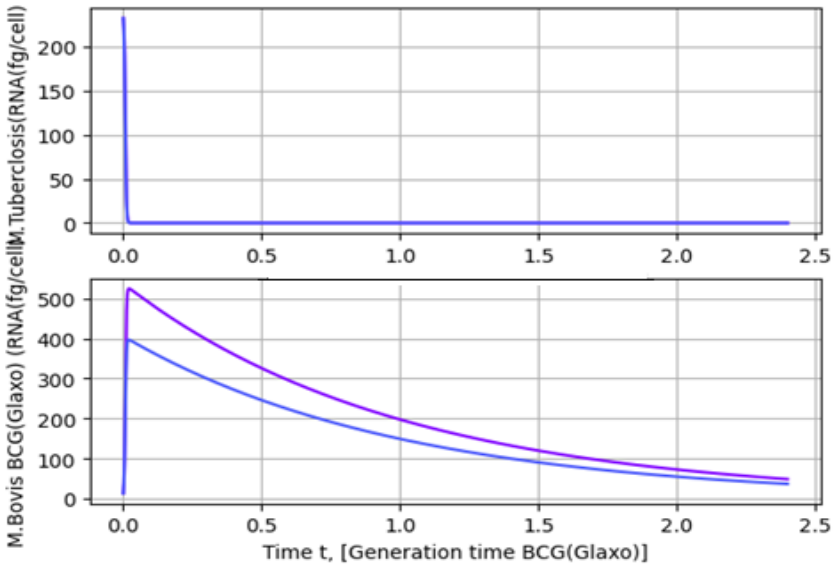

Figure 8 : Interaction of Random Model M. tuberculosis (RNA/fg/cell) and M. bovis BCG Glaxo (RNA/fg/cell)

Generation Time t,days	M. tuberculosis (RNA/fg/cell)	M. bovis BCG Glaxo (RNA/fg/cell)
240	2.32000000e+02	1.33000000e+01
240	2.20703642e+02	3.95586887e+01
240	1.90722401e+02	1.07128381e+02
240	-4.45439739e-11	4.89605233e+01
240	-4.97911525e-11	4.88430416e+01
240	2.32000000e+02	1.33000000e+01
240	2.16933659e+02	3.92565763e+01
240	1.79289445e+02	1.02639024e+02
240	1.30580440e-10	3.69804982e+01
240	2.23545942e-10	3.68917628e+01
240	3.20791575e-10	3.68032403e+01

Table 6: Interaction of Random Model M. tuberculosis (RNA/fg/cell) and M. bovis BCG Glaxo (RNA/fg/cell)

The **figure 8** presents RNA concentration (in fg/cell) over time for two bacterial strains: M. tuberculosis and M. Bovis BCG (Glaxo). In the upper plot, M. tuberculosis exhibits a sharp initial decline in RNA concentration, dropping from a high level at t=0 to a much lower and stable level as time progresses. This suggests that M. tuberculosis undergoes rapid RNA degradation or a decrease in metabolic activity early on, stabilizing quickly. In contrast, the lower plot shows that M. Bovis BCG (Glaxo) also starts with a high RNA concentration, but its decline is more gradual, with the concentration decreasing steadily over time. The two lines in this plot indicate slight variations under different conditions but overall, the decline is less steep than in M. tuberculosis. This comparison suggests that M. Bovis BCG (Glaxo) maintains RNA levels longer possibly indicating differences in their physiological or metabolic processes.

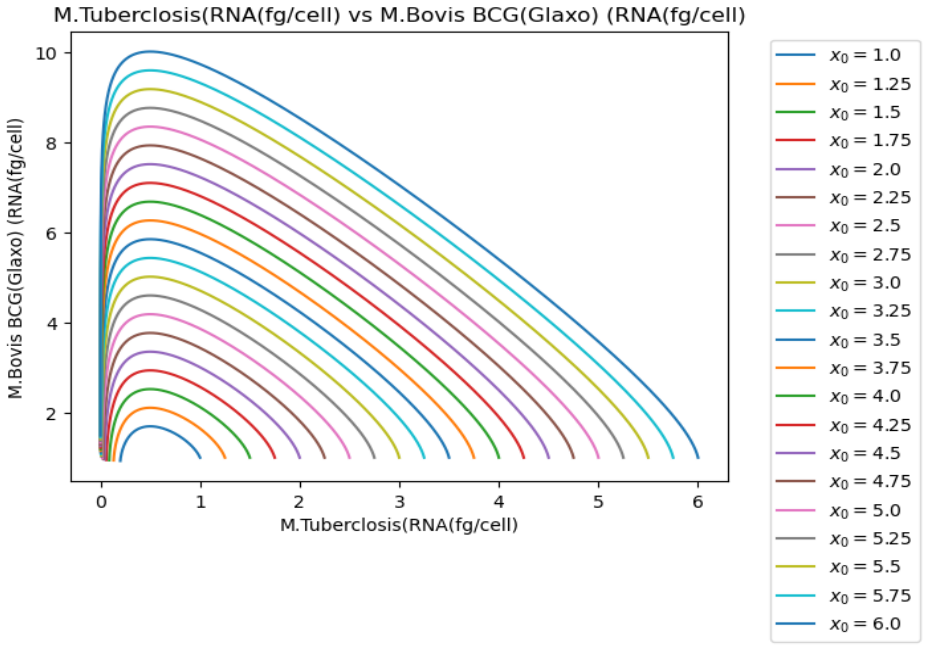

Figure 9: Interaction of Random Model M. tuberculosis (RNA/fg/cell) and M. bovis BCG Glaxo (RNA/fg/cell)

Generation Time t, days	M. tuberculosis (RNA/fg/cell)	M. bovis BCG Glaxo (RNA/fg/cell)
240	2.32000000e+02	1.33000000e+01
240	2.16933659e+02	3.92565763e+01
240	1.79289445e+02	1.02639024e+02
240	1.30580440e-10	3.69804982e+01
240	2.23545942e-10	3.68917628e+01
240	3.20791575e-10	3.68032403e+01

Table 7: Interaction of Random Model M. tuberculosis (RNA/fg/cell) and M. bovis BCG Glaxo (RNA/fg/cell)

In figure 9, The analysis explores the phase plane differences in RNA content per cell (fg/cell) between M. tuberculosis and M. bovis BCG (Glaxo). The x-axis of the graph shows the RNA levels for M. tuberculosis, ranging from 0 to 6 fg/cell, while the y-axis represents the RNA levels for M. bovis BCG (Glaxo), ranging from 0 to 10 fg/cell. Various initial conditions are depicted by colored lines on the graph spanning from $x_0 = 1.0$ to $x_0 = 6.0$. These lines demonstrate how the population of M. bovis BCG (Glaxo) varies in relation to M. M. tuberculosis under different starting scenarios.

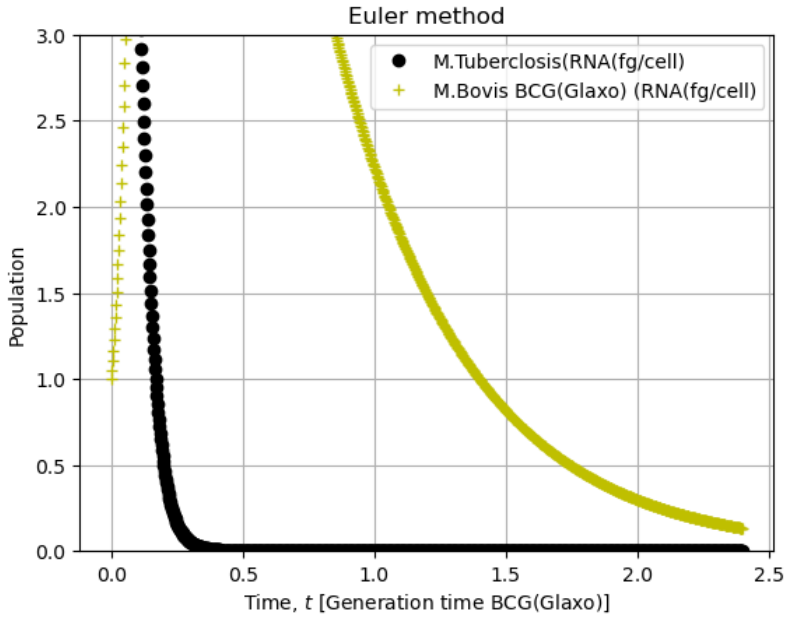

Figure 10: Interaction of Euler Model M. tuberculosis (RNA/fg/cell) and M. bovis BCG Glaxo (RNA/fg/cell)

Generation Time t, days	M. tuberculosis (RNA/fg/cell)	M. bovis BCG Glaxo (RNA/fg/cell)
240	6.00000000e+00	1.00000000e+00
240	5.99423423e+00	1.05285285e+00
240	5.98664734e+00	1.10844079e+00
240	7.35170095e-05	1.36107994e-01
240	7.38125507e-05	1.35454118e-01
240	7.41095582e-05	1.34803384e-01

Table 8: Interaction of Euler Model M. tuberculosis (RNA/fg/cell) and M. bovis BCG Glaxo (RNA/fg/cell)

In **figure 10**, the population of M. tuberculosis and M. bovis BCG(Glaxo) over time measured in Generation time BCG(Glaxo). Here's a brief interpretation. X-Axis (Time): The x-axis represents time measured in Generation time BCG(Glaxo) ranging from 0 to 2.5. Y-Axis (Population): The y-axis represents the population of the bacteria, ranging from 0 to 3.0. M. tuberculosis (Blue Circles): The

blue circles represent the population of M. tuberculosis. The population decreases sharply as time progresses, indicating a decline in the M. tuberculosis population over time. M. bovis BCG(Glaxo) (Green Plus Markers): The green plus markers represent the population of M. bovis BCG(Glaxo). The population remains relatively stable before it too begins to decrease though at a slower rate than M. tuberculosis.

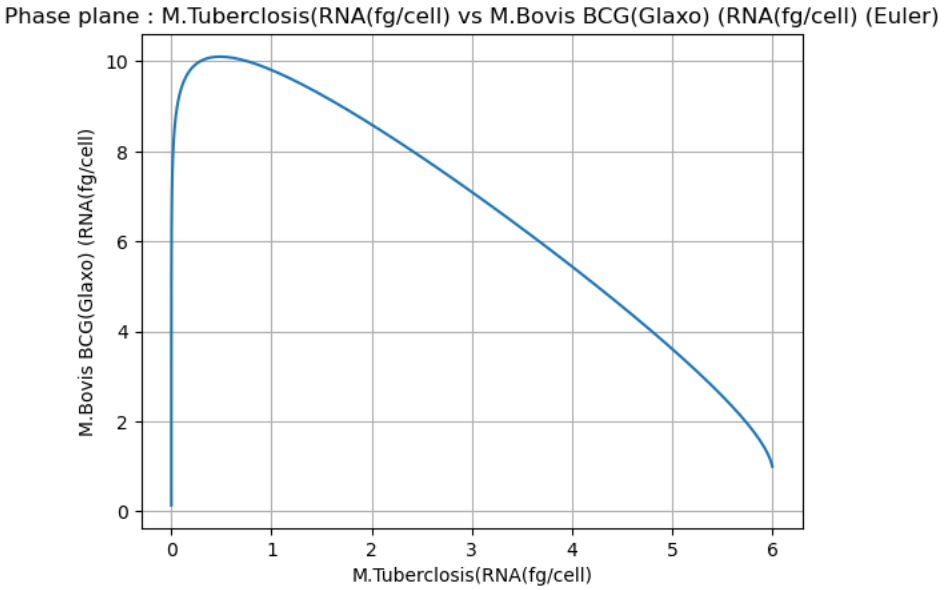

Figure 11: Interaction of Euler Model M. tuberculosis (RNA/fg/cell) and M. bovis BCG Glaxo (RNA/fg/cell)

The **figure11** illustrates a phase plane comparison of M. tuberculosis and M. bovis BCG (Glaxo) based on RNA per cell (fg/cell). The x-axis shows the RNA content of M. tuberculosis, ranging from 0 to 6 fg/cell, while the y-axis represents the RNA content of M. bovis BCG (Glaxo) ranging from 0 to 10 fg/cell. The blue curve on the graph depicts the relationship between these two bacteria. It shows that as the RNA content per cell for M. tuberculosis increases, the RNA content per cell for M. bovis BCG (Glaxo) decreases significantly highlighting an inverse relationship between the two variables.

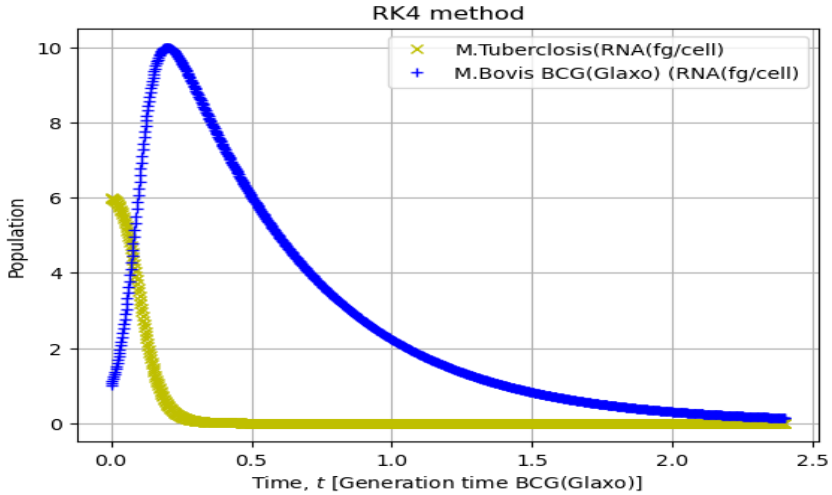

Figure 12: Interaction of RK-Method Model M. tuberculosis (RNA/fg/cell) and M. bovis BCG Glaxo (RNA/fg/cell)

Generation Time BCG (Glaxo) measures the population dynamics of M. tuberculosis and M. bovis over time. The **figure 12** illustrates this relationship with time displayed on the x-axis, ranging from 0 to 2.5 units of Generation Time BCG (Glaxo). The y-axis shows the bacterium's population, ranging from 0 to 10. M. tuberculosis is depicted by blue circles, showing a rapid increase in population that eventually peaks and then declines. In contrast, M. bovis BCG (Glaxo) represented by green plus markers, also experiences population growth but peaks later and at a lower level before decreasing. This comparison highlights the differing growth patterns and peak timings of the two bacterial populations.

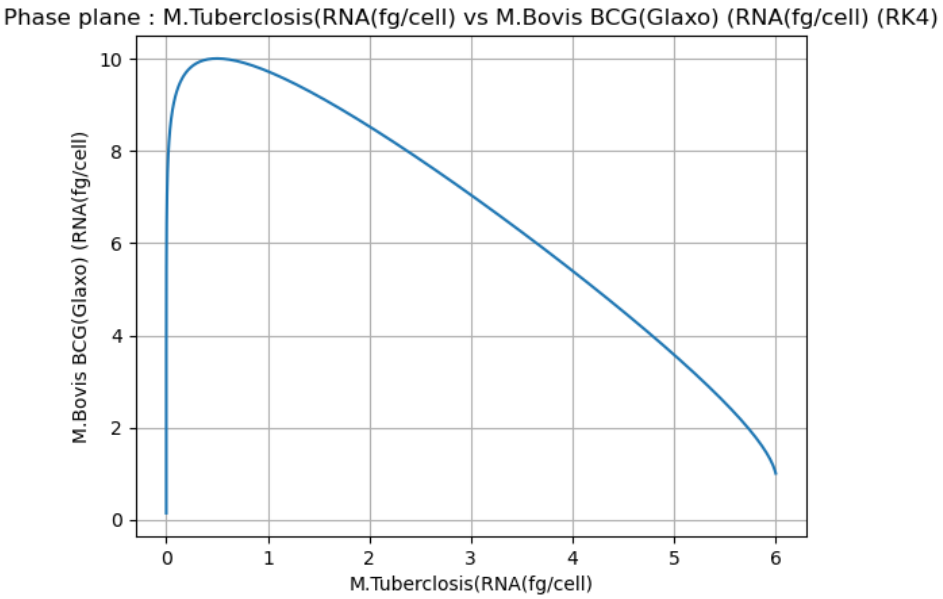

Figure 13: Phase plane: Interaction of RK-Method Model M. tuberculosis (RNA/fg/cell) and M. bovis BCG Glaxo (RNA/fg/cell)

Generation Time t,days	M. tuberculosis (RNA/fg/cell)	M. bovis BCG Glaxo (RNA/fg/cell)
240	6.00000000e+00	1.00000000e+00
240	5.99330780e+00	1.05424217e+00
240	5.98470205e+00	1.11134495e+00
240	9.57159333e-05	1.36713643e-01
240	9.61013355e-05	1.36058461e-01
240	9.64886532e-05	1.35406420e-01

Table 9: Interaction of RK-Method Model M. tuberculosis (RNA/fg/cell) and M. bovis BCG Glaxo (RNA/fg/cell)

In **figure 13**, an analysis of the phase plane differences in terms of RNA per cell (fg/cell) between M. tuberculosis and M. bovis BCG (Glaxo) is done. This is a succinct interpretation. The X-Axis

(M. tuberculosis): 0 to 6 signifies M. tuberculosis (RNA/fg/cell). Y-Axis (M. bovis BCG1): Running from 0 to 10, the y-axis shows M. bovis BCG(Glaxo) (RNA/fg/cell). Blue Curve: This diagram illustrates the connection between M. tuberculosis and M. bovis BCG (Glaxo). M. bovis BCG (Glaxo) RNA per cell falls down dramatically when M. tuberculosis RNA per cell rises. This suggests that there is an inverse link between these two factors.

5. Conclusion

In conclusion, the ODE model offers a robust framework for studying and simulating the biological interactions between M. tuberculosis and Mycobacterium bovis BCG Glaxo. Its versatility allows for adjustments in parameters, initial conditions, boundary conditions, time intervals and numerical methods making it a powerful tool for exploring these dynamics. Whether implemented using different programming languages such as Python or employing various numerical techniques like Euler's method or the Runge-Kutta fourth order, the model remains a crucial asset in biological research. This flexibility underscores the significance of computational models in advancing our comprehension of intricate biological systems and their interactions.

References

[1] Abdallah AM, Hill-Cawthorne GA, Otto TD, Coll F, Guerra-Assunção JA, Gao G, Naeem R, Ansari H, Malas TB, Adroub SA et al. (2015) Genomic expression catalogue of a global collection of BCG vaccine strains show evidence for highly diverged metabolic and cell-wall adaptations. Sci Rep 5:15443.

[2] A.J. Lotka. Elements of Physical Biology. Williams and Wilkins, Baltimore, 1925.

[3] Brosch R, Gordon SV, Garnier T, Eiglmeier K, Frigui W, Valenti P, Dos Santos S, Duthoy S, Lacroix C, Garcia-Pelayo C et al. (2007) Genome plasticity of BCG and impact on vaccine efficacy. Proc Natl Acad Sci U S A 104:5596–5601.

[4] Dr. Neelam Patel, Dr. Vikram Singh (2024) "Mathematical Modeling of Infectious Disease Dynamics: The Role of Vaccination in Disease Control," Mathematical Methods in the Applied Sciences.

[5] Dr. Ravi Kumar, Dr. Anjali Sharma "Mathematical Modeling of M. tuberculosis Dynamics with Intervention Strategies," Journal of Mathematical Biology and Applied Sciences.

[6] E. Juarlin (2019) J. Phys.: Conf. Ser. 1341 062024

[7] Edson NL. The intermediary metabolism of the mycobacteria. Bacteriol Rev. (1951); 15: 147–182. [PubMed: 14886295]

[8] Gunasekaran. M and Alamelu K (2023) Enhancing M. tuberculosis Modeling: The True Positive Vaccinated Approach Utilizing a Specialized Runge-Kutta Method. Journal of Harbin Engineering University ISSN: 1006-7043 Vol 44 No. 11.

[9] Gunasekaran. M and Alamelu K (2023) Comparative Exploration of M. tuberculosis in High-Risk and Low-Risk Population by Enhanced Numerical Algorithm. Journal of Advanced Zoology, Volume 44 Issue S8 Year 2023 Page 430441, ISSN: 0253-7214.

[10] M. Gunasekaran and A. M. Sarravanaprabhu, "Optimal harvesting of three species dynamic model with bionomic equilibrium", Turkish Journal of Computer and Mathematics Education, vol. 11, no. 3, pp. 1339–1350, 2020.

[11] M. Gunasekaran and A. M. Sarravanaprabhu, "A second type of Holling functional response of stability analysis for prey-predator and host ecosystem", Advances and Applications in Mathematical Sciences, vol. 21, no. 11, pp. 6213–6233, Sep. 2022.

[12] M. Gunasekaran and A. M. Sarravanaprabhu, "An analysis of stability behaviour for two preys and two predators ecological model", Journal of Advanced Zoology, vol. 44, no. S-8, pp. 442–462, 2023.

[13] M. Gunasekaran and A. M. Sarravanaprabhu, "A mathematical analysis of refuge, migration and immigration effects on predator-prey dynamics", Nanotechnology Perceptions, vol. 20, no. 6, pp. 3468–3487, 2024.

[14] Keating LA, Wheeler PR, Mansoor H, Inwald JK, Dale J, Hewinson RG, Gordon SV. The pyruvate requirement of some members of the Mycobacterium M. tuberculosis complex is due to an inactive pyruvate kinase: implications for in vivo growth. Mol Microbiol. (2005); 56: 163–174. [PubMed: 15773987]

[15] Ratledge C. The physiology of the mycobacteria. Adv Microb Physiol. (1976); 13:115–244. [PubMed: 775942]

[16] Ratledge C, Dover LG. Iron metabolism in pathogenic bacteria. Annu Rev Microbiol. (2000); 54:881–941. [PubMed: 11018148]

[17] Ratledge C. Nutrition, growth and metabolism. In: Ratledge, C.; Stanford, J., editors. The biology of the mycobacteria. Academic Press, Ltd; London, United Kingdom: (1982). p. 186-212.

[18] Ramakrishnan T, Murthy PS, Gopinathan KP. Intermediary metabolism of mycobacteria. Bacteriol Rev. (1972); 36:65–108. [PubMed: 4553808]

[19] Sujatha. K, Gunasekaran. M (2015). Two Ways of Stability Analysis of Prey-Predator System with Diseased Prey Population. The International Journal of Engineering and Science (IJES), Volume-4, Issue-7, Pages 61-66, ISSN (e): 2319–1813 ISSN (p): 2319–1805.

[20] S. Sundararajan, P. Murugan, M. S. R. Jayaraman (2023) "Mathematical Modeling and Analysis of M. tuberculosis with Vaccination Strategies", International Journal of Mathematical Sciences and Computing.

[21] Wheeler, PR.; Blanchard, JS. General metabolism and biochemical pathways of tubercle bacilli. In: Cole, ST.; Davis Eisenach, K.; McMurray, DN.; Jacobs, WR., Jr, editors. M. tuberculosis and the Tubercle Bacillus. ASM Press; Washington, D.C: (2005). p. 309-339.

[22] Zhang W, Zhang Y, Zheng H, Pan Y, Liu H, Du P, Wan L, Liu J, Zhu B, Zhao G et al. (2013) Genome sequencing and analysis of BCG vaccine strains.